Supporting Information

Weisbrod et al. 10.1073/pnas.1221022110

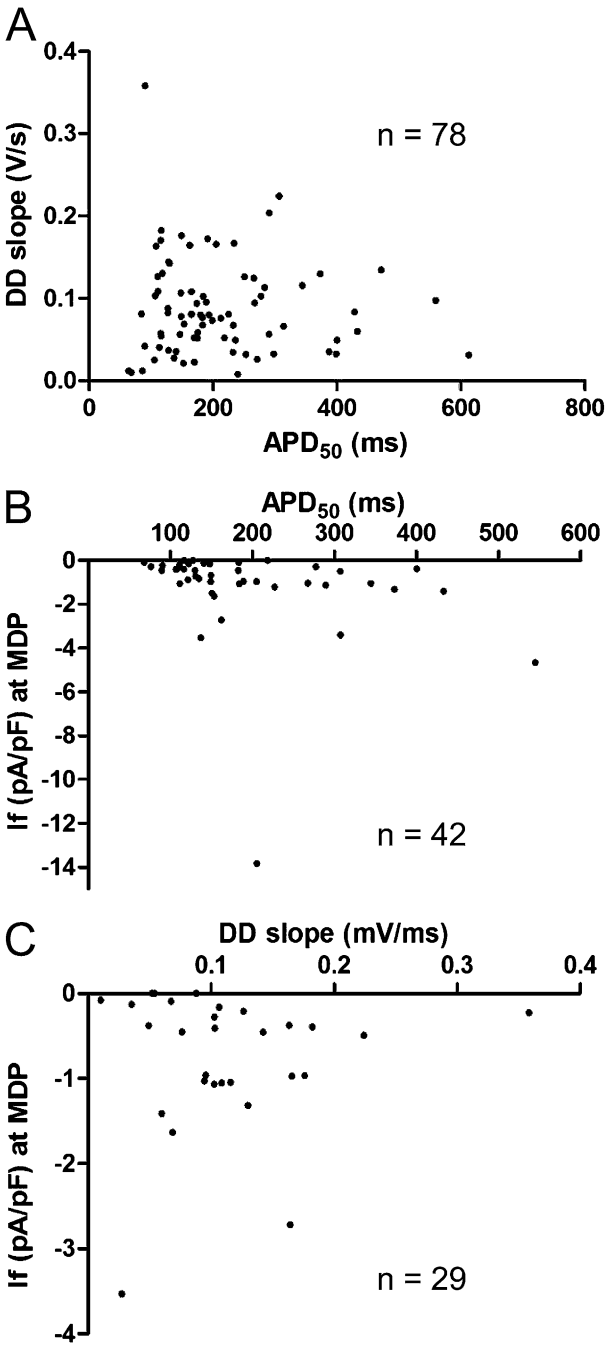

Fig. S1. Lack of correlation in the relations between the AP duration at 50% repolarization (APD_{50}), the diastolic depolarization (DD) slope, and funny current (I_f) current density. (*A*) No correlation was found between the DD slope and APD_{50} (r = −0.055, $P = 0.628$, $n = 78$). (*B*) No correlation was found between the I_f current density measured at MDP and APD_{50} (r = −0.239, $P = 0.127$, $n = 42$). (*C*) No correlation was found between the I_f current density measured at MDP and the DD slope ($r = 0.065$, $P = 0.736$, n =29).

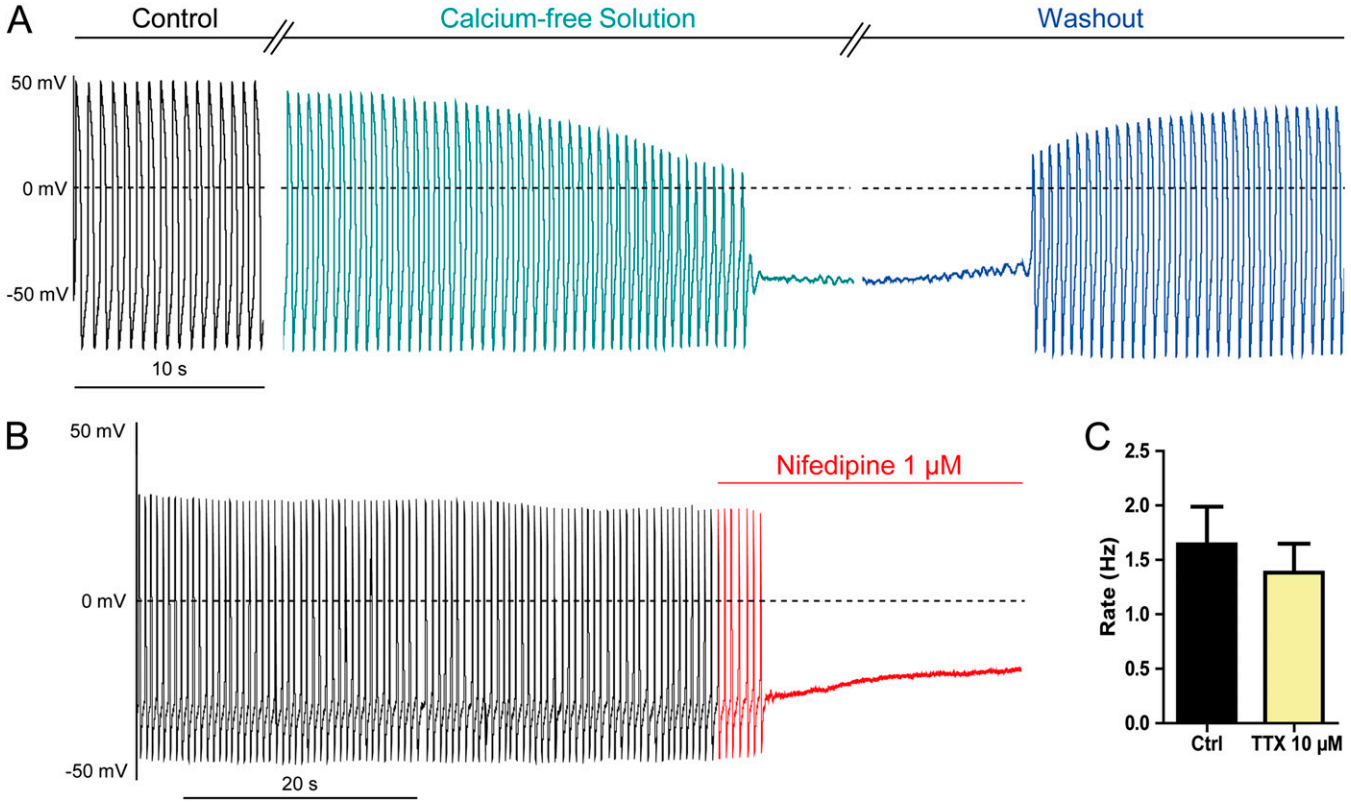

Fig. S2. Effect of external Ca^{2+}-free solution and nifedipine on early (11–21 d in vitro) stage-derived human embryonic stem cell-derived cardiomyocyte (hESC-CM) automaticity. (*A*) Representative trace of a spontaneously beating hESC-CM exposed to an external Ca^{2+}-free recording solution and followed by a washout. (*B*) Representative trace of a spontaneously beating hESC-CM treated with the L-type Ca^{2+} channel blocker nifedipine (1 μM). For both *A* and *B*, five additional experiments gave similar results ($n = 6$). (*C*) Data summary showing the lack of effect of 10 μM tetrodotoxin (TTX) on the beating frequency of young hESC-CMs ($n = 6$).

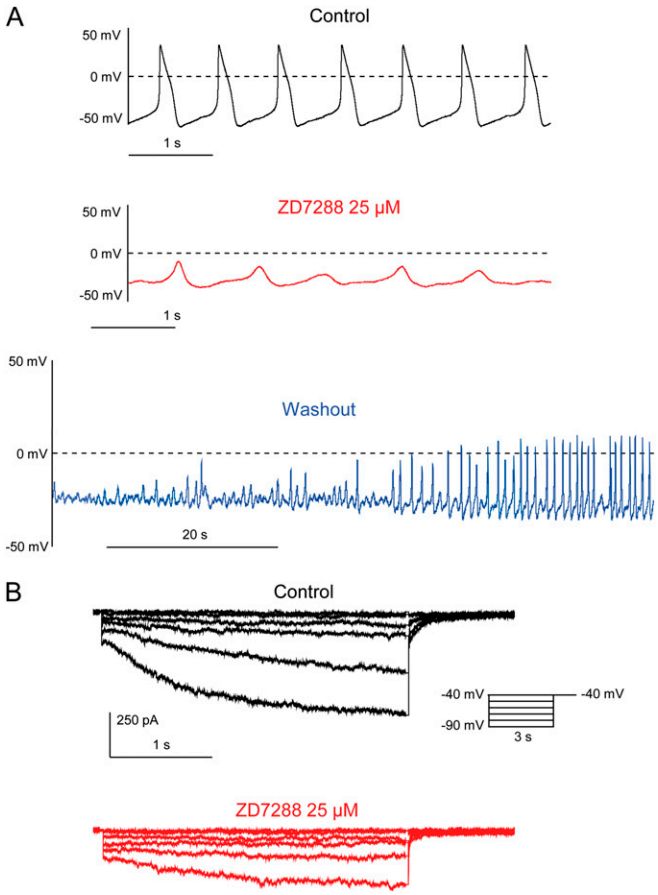

Fig. S3. A subset of hESC-CMs with prominent I_f-dependent pacemaker are sensitive to ZD7288. (*A* and *B*) Combined current- and voltage-clamp recordings were performed in the same cell. (*A*, *Top*) Spontaneous action potential (AP) pattern of an hESC-CM recorded under current-clamp in control conditions (black trace). (*B*) The I_f current was subsequently recorded in the same cell, under voltage-clamp, in the absence (black traces) and presence of 25 μM ZD7288 (red traces) by stepping the membrane from a holding potential of −40 mV to −90 mV in 10-mV decrements for 3 s pulse duration. Once I_f current inhibition by ZD7288 was monitored under voltage-clamp, the AP pattern of the same cell was examined under current-clamp, during continuous ZD7288 exposure (see *A*, *Middle* red trace). Note the complete suppression of the pacemaker activity. The same cell was washed out and partially recovered its pacemaker activity (see *A*, *Bottom* blue trace).

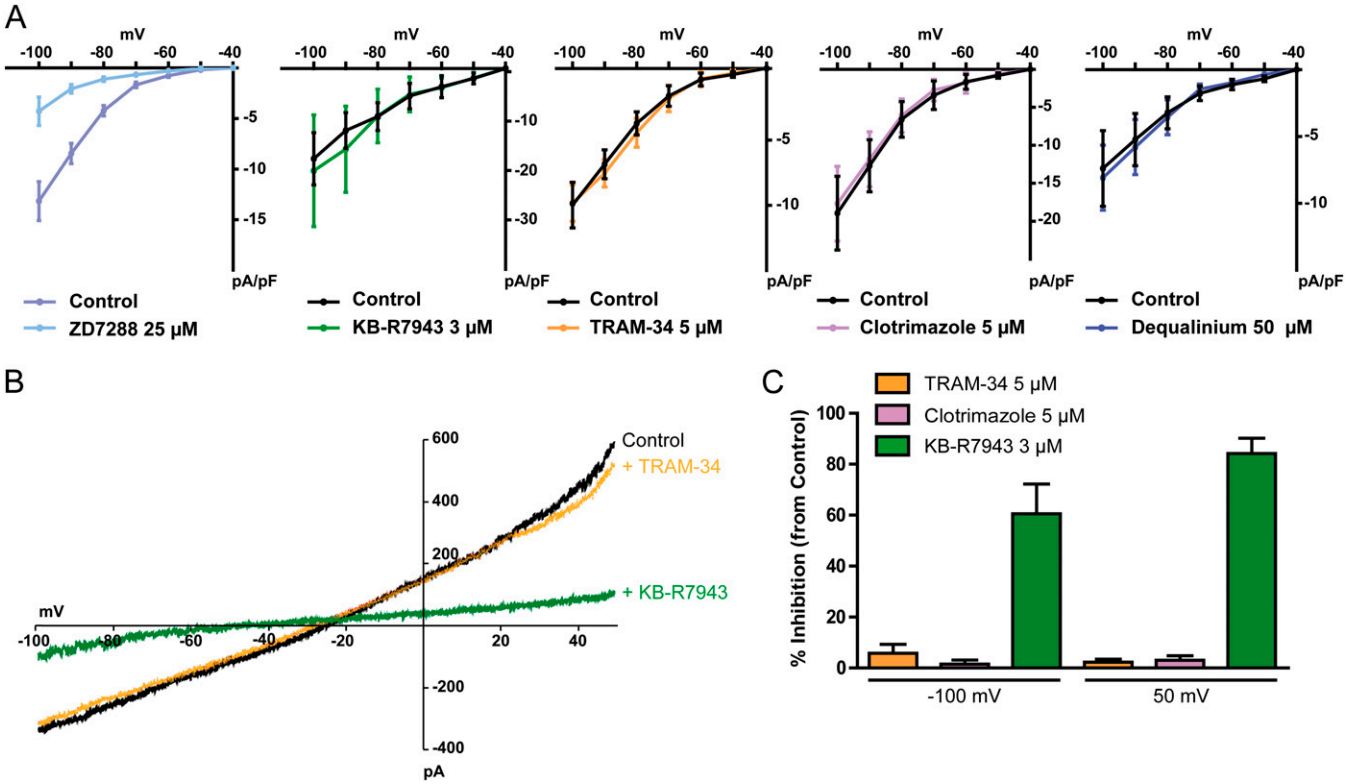

Fig. S4. Sensitivity of the I_f and I_{NCX} currents to the drugs targeting the Ca^{2+}-activated intermediate K^+ conductance (IK_{Ca}, SK4) channel. (*A*) The sensitivity of the I_f current to the drugs was determined in the same hESC-CM in the absence (control) and presence of 25 μM ZD7288, 3 μM KB-R7943, 5 μM 1-[(2-chlorophenyl)-diphenylmethyl]-1H-pyrazole (TRAM 34), 5 μM clotrimazole, or 50 μM dequalinium. Cells were held at −40 mV, and the membrane voltage was stepped from −40 mV to −100 mV (n = 3–9). (*B*) Representative traces showing in the same cell the sensitivity of the I_{NCX} current before and after exposure to 5 μM TRAM 34, followed by washout and exposure to 3 μM KB-R7943. A voltage ramp protocol was performed from +50 mV to −100 mV for 215 ms (*Materials and Methods*). (*C*) The effects of 3 μM KB-R7943, 5 μM TRAM 34, and 5 μM clotrimazole were examined using the voltage ramp protocol and quantified as percentage of inhibition from control at −100 mV and +50 mV (n = 3–9).

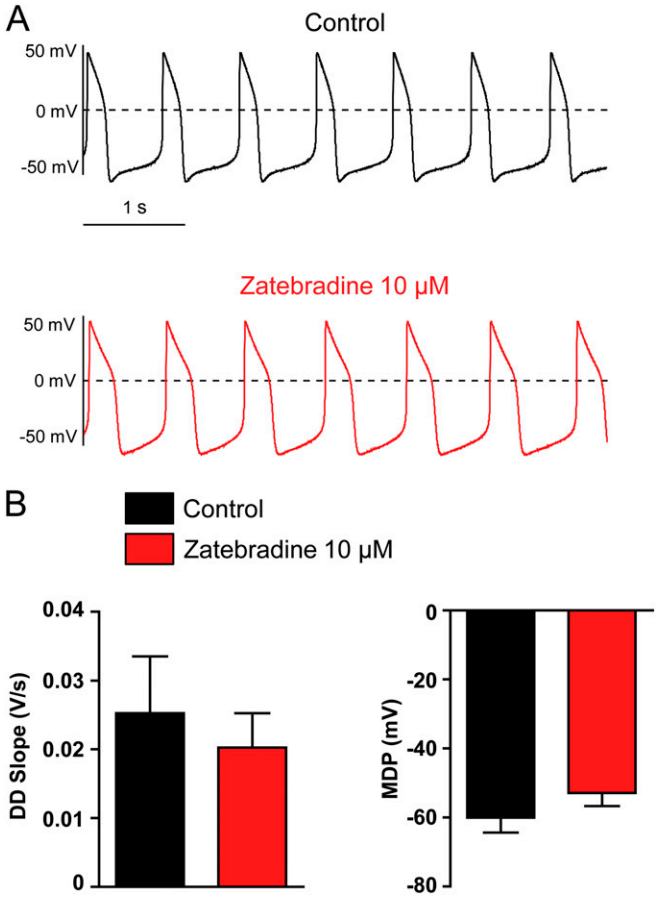

Fig. S5. A subset of hESC-CMs with prominent I_f-independent pacemaker is insensitive to zatebradine. (*A*) Spontaneous AP pattern of an hESC-CM recorded under current-clamp before (control, black trace) and following treatment with 10 μM zatebradine (red trace). (*B*) Zatebradine (10 μM) affects neither the DD Slope nor the maximal diastolic potential (MDP) in this group of hESC-CMs ($n = 4$).

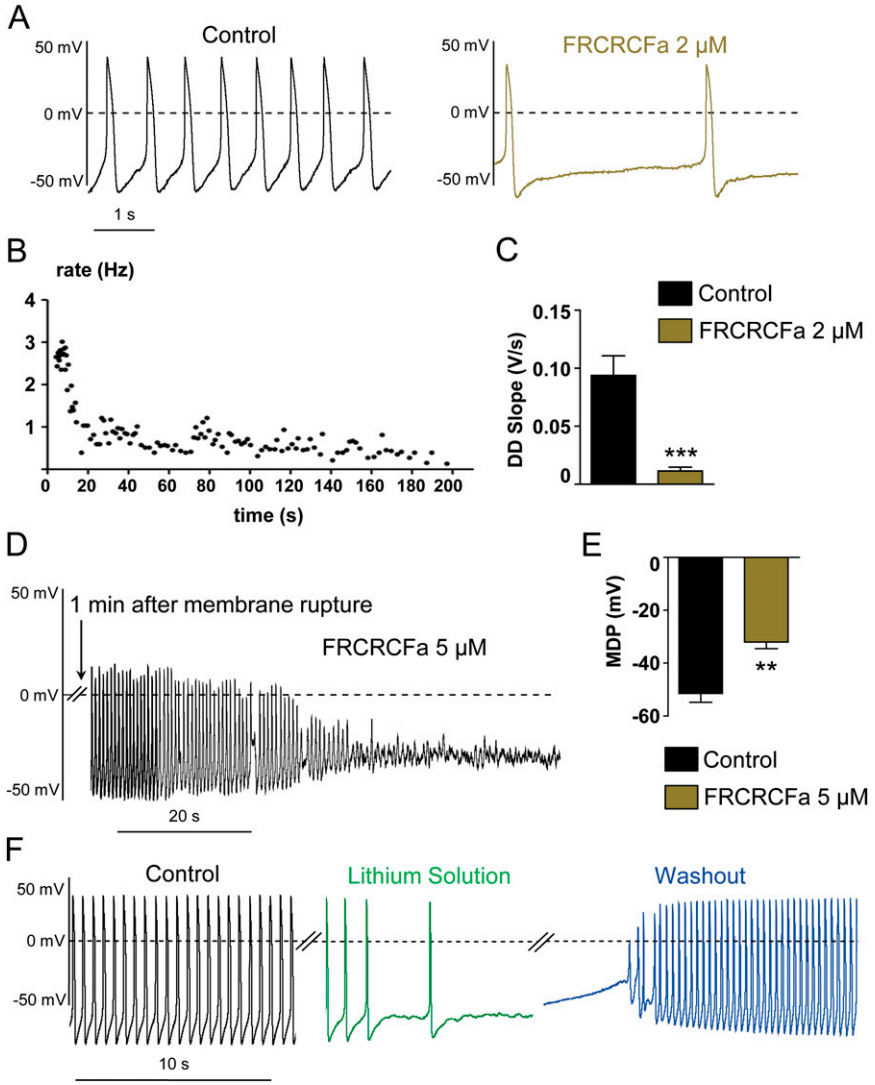

Fig. S6. A subset of hESC-CMs exhibits a pacemaker prominently sensitive to the Na^+–Ca^{2+} exchanger (NCX) blocker Phe-Arg-Cys-Arg-Cys-Phe-CONH2 (FRCRCFa). (*A*) Spontaneous AP pattern of an hESC-CM recorded under current-clamp before (control, black trace) and following treatment with 2 μM FRCRCFa (brown trace). Note, the bradycardia and the decrease in the late DD slope. (*B*) Bradycardia was measured over time (s) by the instantaneous frequency between two contiguous APs (in Hz) following membrane rupture. FRCRCFa (2 μM) was included in the patch pipet. (*C*) FRCRCFa (2 μM) significantly decreased the DD slope (***$P = 0.0001$, $n = 12$). (*D*) Example of a trace showing the spontaneous AP pattern of a cell, about 1 min following membrane rupture, where FRCRCFa (5 μM) was included in the patch pipet. (*E*) FRCRCFa (5 μM) significantly depolarized the MDP (**$P = 0.0032$, $n = 5$) in this subset of cells. (*F*) Spontaneous AP pattern of a hESC-CM recorded under current-clamp before (control, black trace) and following isomolar replacement of external Na^+-containing (140 mM NaCl) solution by Li^+-containing solution (140 mM LiCl) (green trace). This treatment leads to MDP depolarization and cessation of AP. This effect could be reversed upon washout with an external Na^+-containing solution (blue trace). This experiment was repeated five times and gave similar results ($n = 5$).

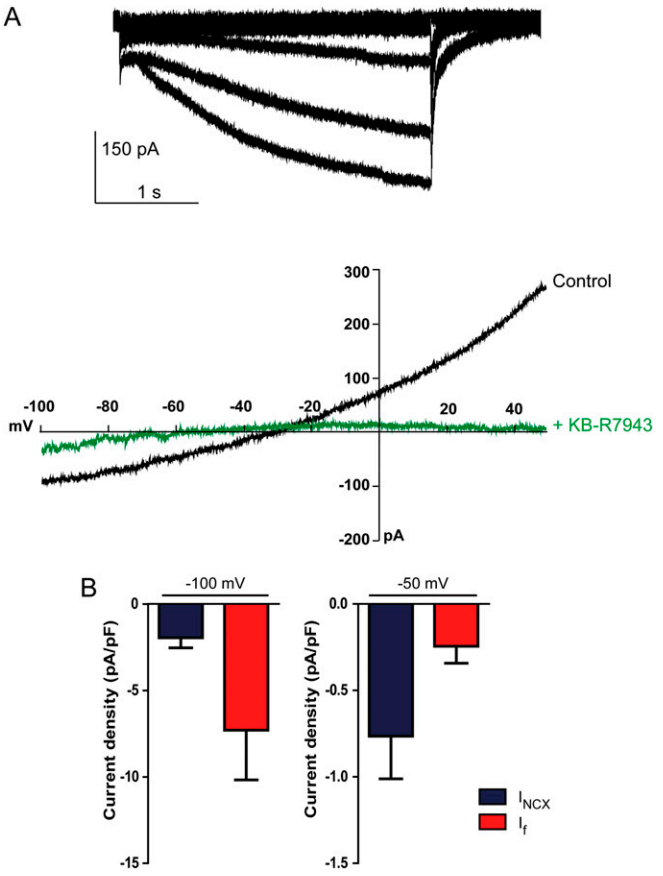

Fig. S7. Comparison of the I_f and I_{NCX} current densities in the same hESC-CMs. (*A*) Representative current traces of I_f (*Upper*) and of I_{NCX} current (*Lower*) recorded as described in Fig. S4. (*B*) The I_f and I_{NCX} current densities were determined at −100 mV and −50 mV and quantified as pA/pF ($n = 5$).

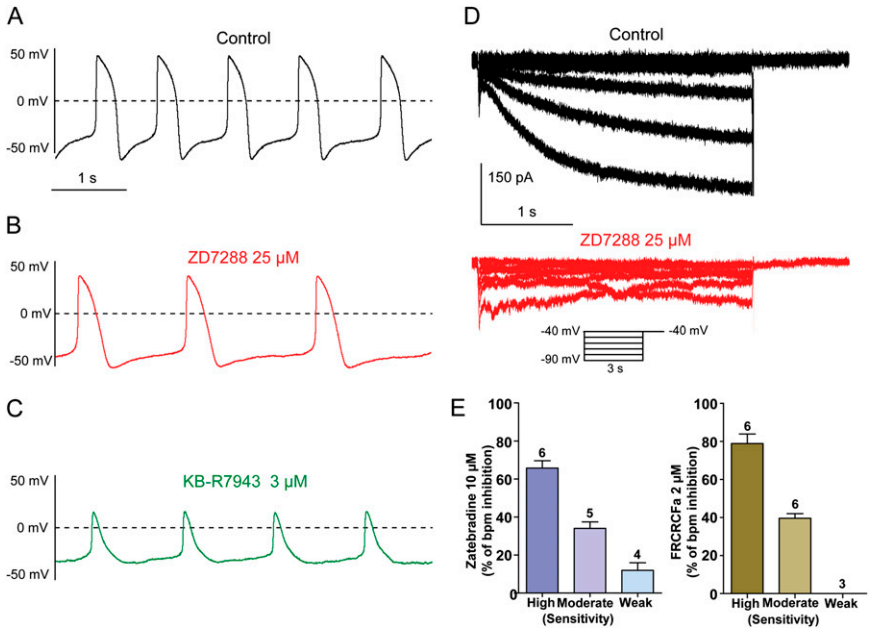

Fig. S8. hESC-CM displaying both I_f-dependent and I_f-independent pacemakers. (*A–D*) Combined current- and voltage-clamp recordings were performed in the same cell. (*A*) Spontaneous AP pattern of an hESC-CM recorded under current-clamp in control conditions (black trace). (*B*) Once I_f current inhibition by ZD7288 was monitored under voltage-clamp (see *D*), the AP pattern of the same cell was examined under current-clamp, during continuous ZD7288 exposure (red trace). Note the bradycardia and the notch suppression at early DD; however, no complete suppression of pacemaker activity was reached. (*C*) After ZD7288 washout, the same cell was exposed to 3 µM KB-R7943, which led to depression of the DD slope and the pacemaker (green trace). (*D*) The I_f current was recorded in the same cell, under voltage-clamp, in the absence (black traces) and presence of 25 µM ZD7288 (red traces) by stepping the membrane from a holding potential of −40 mV to −90 mV in 10-mV decrements for 3 s pulse duration. (*E*) One can distinguish three categories of cells responsive to zatebradine (I_f) and FRCRCFa (NCX), with respect to their inhibition of AP frequency; hESC-CMs highly (50–100% inhibition), moderately (25–50% inhibition), and weakly (0–25% inhibition) sensitive to zatebradine or FRCRCFa. All three categories were significantly different from each other (ANOVA followed by Tukey's Multiple Comparison Test; $P < 0.0001$). All drug-sensitive categories were significantly different from their control, except for the FRCRCFa weakly-sensitive group ($P < 0.05$).

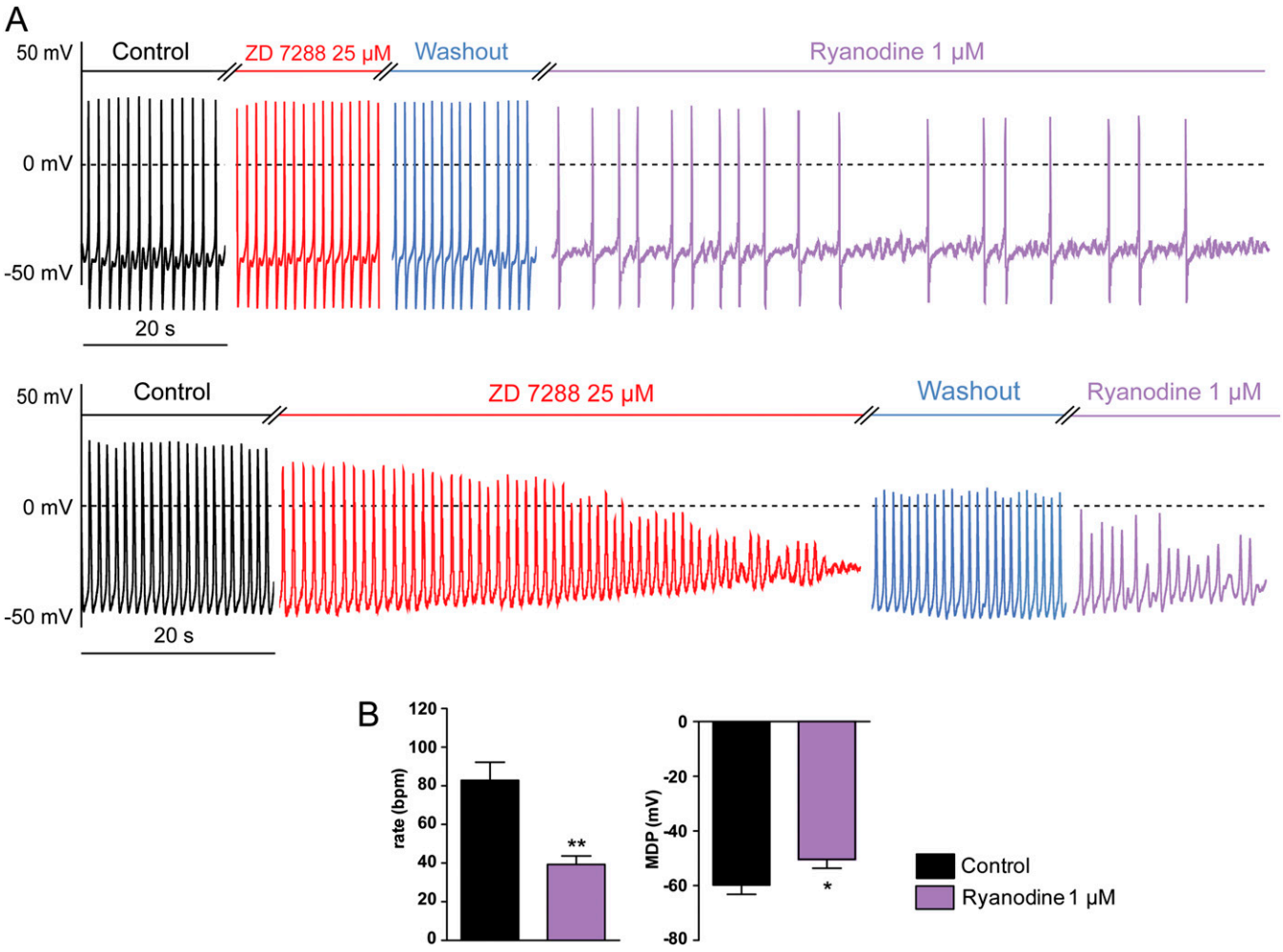

Fig. S9. The pacemaker of both I_f-dependent and I_f-independent hESC-CMs is highly sensitive to ryanodine. (*A*) The *Upper* panel shows the spontaneous AP pattern of an hESC-CM insensitive to 25 μM ZD7288 exposure (I_f-independent), which after washout was sensitive to 1 μM ryanodine, producing bradycardia and the ultimate vanishing of APs. The *Lower* panel shows the spontaneous AP pattern of an hESC-CM sensitive to 25 μM ZD7288 exposure (I_f-dependent), which after washout was sensitive to 1 μM ryanodine, producing MDP depolarization and vanishing of APs. (*B*) Ryanodine significantly depressed the AP frequency (**$P = 0.0010$, $n = 5$) and depolarizes the MDP (*$P = 0.039$, $n = 5$).

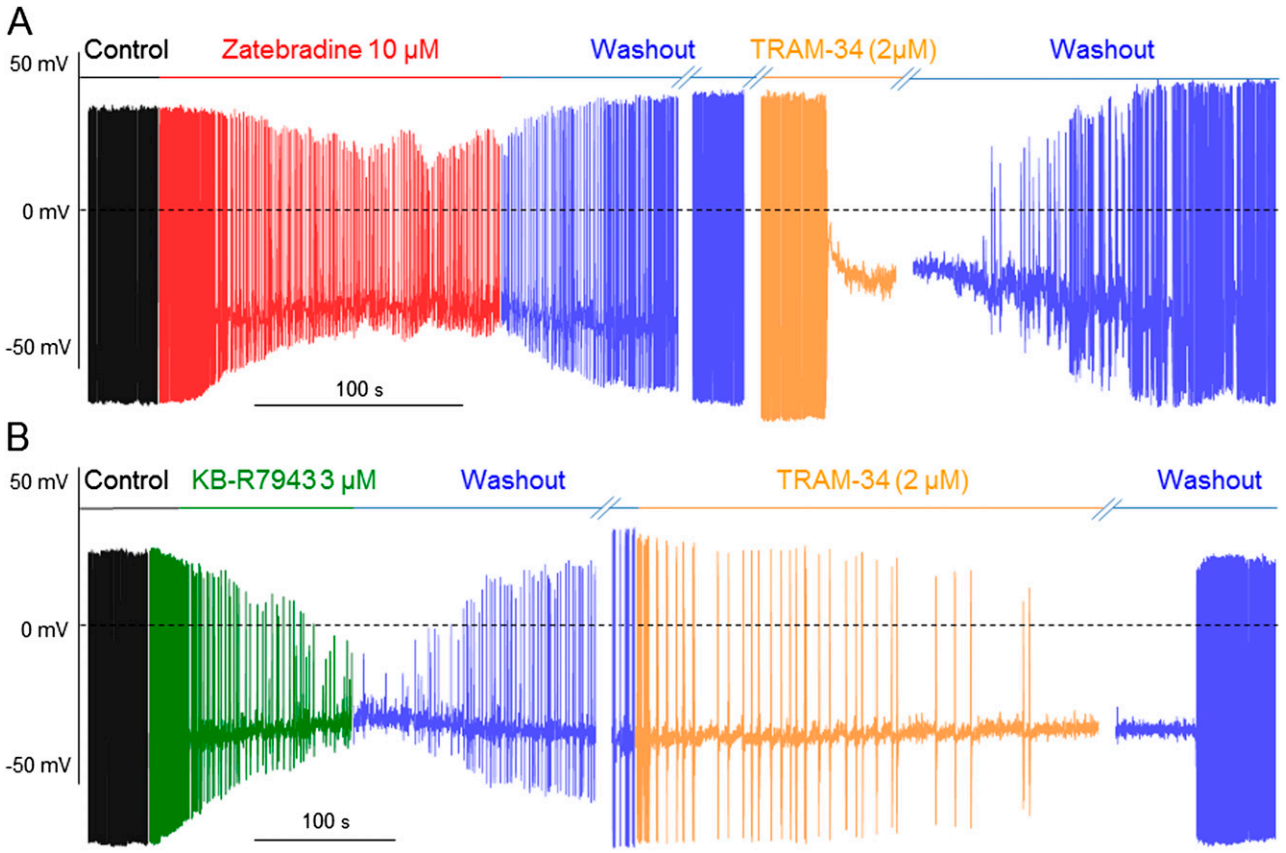

Fig. S10. TRAM 34 inhibits both I_f-dependent and I_f-independent pacemakers. (*A*) Representative spontaneous AP pattern of an hESC-CM with I_f-dependent pacemaker recorded in control conditions (black trace). Then, the same cell was treated with the I_f blocker zatebradine (10 μM) (red trace). Note the bradycardia and the MDP depolarization. Subsequently, the cell was washed out (blue trace) and treated with TRAM 34 (2 μM) (orange trace), which led to an abrupt cessation of AP that was reversible by washout (blue trace). (*B*) Representative spontaneous AP pattern of another hESC-CM with I_f-independent pacemaker recorded in control conditions (black trace). Then, the same cell was treated with the NCX blocker KB-R7943 (3 μM) (green trace). Note the bradycardia and the MDP depolarization, which nearly caused a cessation of AP. Subsequently, the cell was washed out (blue trace) and treated with TRAM 34 (2 μM) (orange trace), which led to a progressive bradycardia, MDP depolarization, and cessation of AP that was reversible by washout (blue trace).

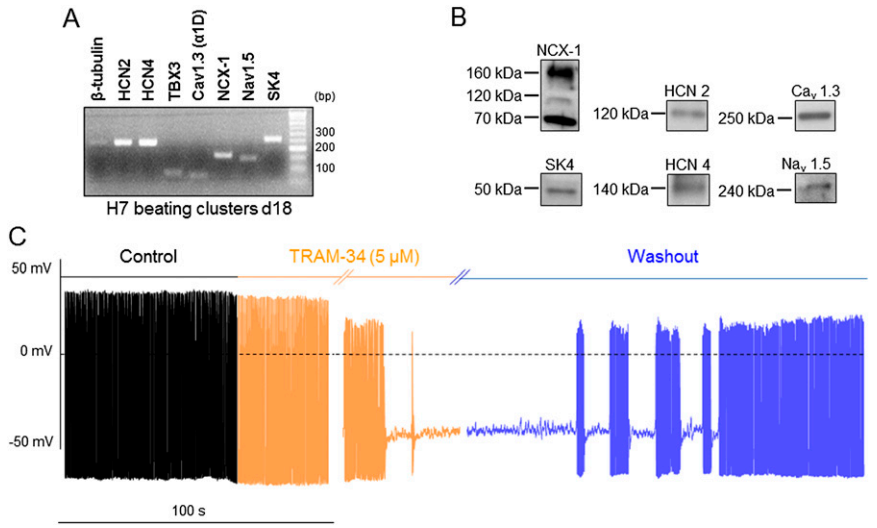

Fig. S11. Characterization of SK4 channels and their impact on pacemaker activity in young (15–18 d in vitro) hESC-CMs derived from the H7 human ES cell line. (*A*) Representative agarose gel of an RT-PCR experiment performed in an early stage-derived embryoid body (EB) (18 d in vitro) and showing bands of derived transcripts encoding β tubulin, hyperpolarization-activated cyclic nucleotide-gated ion channel (HCN)2, HCN4, T-box protein 3, voltage-gated Ca^+ channel 1.3 (isoform α1D) [Cav1.3 (α1D)], NCX1, voltage-gated Na^+ channel 1.5 (Nav1.5), and SK4 genes. (*B*) Western blots showing immunoreactive bands of HCN2, HCN4, Cav1.3 (α1D), NCX1, Nav1.5, and SK4 proteins in 18-d-old beating EBs. (*C*) Spontaneous fast beating pattern of an early stage (9 d in vitro) H7-derived hESC-CM recorded under current-clamp before (control, black trace) and following treatment with 5 μM TRAM 34 (orange trace), which led to MDP depolarization and cessation of automaticity. This effect could be washed out (blue trace). This experiment was repeated five times and yielded similar results ($n = 6$).

Table S1. Primer list

Name	Forward and reverse sequences	Length, bp
SK4_4	Fwd: GGA CAT CTC CAA GAT GCA CA	249
(KCNN4) NM_002250	Rev: AGG AGT GGC AGA GAC GAT GT	
TBX3	Fwd: CCTGGAGGCTAAAGAACTTTGGGA	85
NM_005996	Rev: AGGAAACATTCGCCTTCCCGACTT	
HCN2	Fwd: CGCCTGATCCGCTACATCCAT	226
NM_001194	Rev: AGTGCGAAGGAGTACAGTTCACT	
HCN4	Fwd: CCCGCCTCATTCGATATATTCAC	233
NM_005477	Rev: GAGCGCGTAGGAGTACTGCTTC	
Cav1.3 (α1D)	Fwd: TCCAAGGAGACGCCTACTACCT	73
NM_005477	Rev: GCGCAGGCACTCAAAGTTG	
Nav1.5	Fwd: CAAGACCTGCTACCACATCGTG	145
NM_198056	Rev: GTCGGCATACTCAAGCAGAACC	
NCX1	Fwd: AAAGAGGAAGAGGAGAGGCGCATT	163
(NM_001112801)	Rev: TCCAGCTGTTAGTCCCAACCACAA	
β-TUBULIN	Fwd: CCGGACAGTGTGGCAACCAGATCG	223
(NM_178014)	Rev: TGGCCAAAAGGACCTGAGCGAACGG	